A novel algorithm based on DFB tunable laser array for demodulation of FBG sensors

Yu Guo[1,2a]**, Huixuan Yao**[1]**, Haodong Wu**[2]**, and Yi Ni**[1]

[1] *School of Internet of Things Engineering, Jiangnan University,*
No. 1800 Lihu Avenue, Wuxi, Jiangsu, 214122, People's Republic of China
[2] *Nanjing University,*
No. 22, Hankou Road, Nanjing, Jiangsu 210093, People's Republic of China
a) *guoynju@163.com*

Abstract: In this paper, a high effective demodulate algorithm based on tunable four-channel DFB (Distributed Feedback) laser array is proposed. In comparison with common algorithms which can work correctly when tunable laser have to be rapidly tuned through FBG's (Fiber Bragg Grating) whole spectrum, the algorithm is unique in that accurate demodulation can be done by scanning only 0.4 nm bandwidth of FBG's reflected spectrum and the scanned spectrum can be any part of the whole FBG spectrum including those regions with relatively low power. Therefore, the laser tuning time and response time of demodulation system is much more reduced which is important for most applications that need dynamic, real-time measurements. Wavelength-division multiplexing for FBG sensing network will be supported by the demodulating system and algorithm. Based on strain experiments of the FBG sensing system, excellent demodulation accuracy were demonstrated by the proposed algorithm.

Keywords: demodulation algorithm, tunable laser array, FBG, WDM
Classification: Optical systems

References

[1] B. Torres, *et al.*: "Analysis of the strain transfer in a new FBG sensor for structural health monitoring," Eng. Struct. **33** (2011) 539 (DOI: 10.1016/j.engstruct.2010.11.012).
[2] Z. Zhou, *et al.*: "Intelligent monitoring and diagnosis for modern mechanical equipment based on the integration of embedded technology and FBGs technology," Measurement **44** (2011) 1499 (DOI: 10.1016/j.measurement.2011.05.018).
[3] J. Dai, *et al.*: "Optical hydrogen sensor based on etched fiber Bragg grating sputtered with Pd/Ag composite film," Opt. Fiber Technol. **19** (2013) 26 (DOI: 10.1016/j.yofte.2012.09.006).
[4] W. Huang, *et al.*: "A cross-correlation method in wavelet domain for demodulation of FBG-FP static-strain sensors," IEEE Photonics Technol. Lett. **26** (2014) 1597 (DOI: 10.1109/LPT.2014.2327969).
[5] J. Liu, *et al.*: "A demodulation method of FBG based on DFB laser and PID algorithm," 2011 Academic International Symposium on Optoelectronics and Microelectronics Technology (2011) 219 (DOI: 10.1109/AISMOT.2011.

DOI: 10.1587/elex.14.20170955
Received September 16, 2017
Accepted September 26, 2017
Publicized October 12, 2017
Copyedited October 25, 2017

6159358).
[6] L. S. Yan, *et al.*: "A simple demodulation method for FBG temperature sensors using a narrow band wavelength tunable DFB laser," IEEE Photonics Technol. Lett. **22** (2010) 1391 (DOI: 10.1109/LPT.2010.2060478).
[7] J. Mo, *et al.*: "A fast tunable semiconductor laser for FBG sensor interrogation systems," 2014 IEEE SENSORS (2014) 1348 (DOI: 10.1109/ICSENS.2014.6985261).
[8] M. S. Muller, *et al.*: "Fiber-optic sensor interrogation based on a widely tunable monolithic laser diode," IEEE Trans. Instrum. Meas. **59** (2010) 696 (DOI: 10.1109/TIM.2009.2025987).
[9] A. Theodosiou, *et al.*: "Modified fs-laser inscribed FBG array for rapid mode shape capturing of free-free vibrating beams," IEEE Photonics Technol. Lett. **28** (2016) 1509 (DOI: 10.1109/LPT.2016.2555852).
[10] C. Massaroni, *et al.*: "Medical smart textiles based on fibre optic technology: an overview," J. Funct. Biomater. **6** (2015) 204 (DOI: 10.3390/jfb6020204).
[11] S. Poeggel, *et al.*: "Recent improvement of medical optical fibre pressure and temperature sensors," Biosensors **5** (2015) 432 (DOI: 10.3390/bios5030432).
[12] J. Hou, *et al.*: "A method of adjusting wavelengths of distributed feedback laser arrays by injection current tuning," IEEE Photon. J. **4** (2012) 2189 (DOI: 10.1109/JPHOT.2012.2228183).
[13] Y. T. Zhou, *et al.*: "Dual current injection tunable SBG semiconductor laser with asymmetric π equivalent phase shift," Microw. Opt. Technol. Lett. **55** (2013) 692 (DOI: 10.1002/mop.27357).
[14] J. S. Li, *et al.*: "Experimental demonstration of distributed feedback semiconductor lasers based on reconstruction-equivalent-chirp technology," Opt. Express **17** (2009) 5240 (DOI: 10.1364/OE.17.005240).
[15] Y. C. Shi, *et al.*: "Study of multiwavelength DFB semiconductor laser array with asymmetric structures based on sampling technique," Appl. Opt. **53** (2014) 6804 (DOI: 10.1364/AO.53.006804).
[16] W. R. Allan, *et al.*: "Multiplexed fiber Bragg grating interrogation system using a microelectromechanical Fabry–Perot tunable filter," IEEE Sensors J. **9** (2009) 936 (DOI: 10.1109/JSEN.2009.2024849).
[17] Z. L. Xu, *et al.*: "A fiber volume strain sensor based on Mach-Zehnder Interferometer," IEEE SENSORS (2012) 1 (DOI: 10.1109/ICSENS.2012.6411459).
[18] J. Zhang and H. Zhao: "Matched FBG application research on dynamic sensing and demodulation," Symposium on Photonics and Optoelectronics (2009) 1 (DOI: 10.1109/SOPO.2009.5230236).
[19] N. S. Aulakh and R. S. Kaler: "Fiber Bragg grating interrogator using edge filtering technique with microbend loss error mitigation," Optik **122** (2011) 796 (DOI: 10.1016/j.ijleo.2010.06.003).

1 Introduction

Fiber Bragg Grating based sensing system has been used in many applications including civil and structure engineering, transportation engineering and aviation industry [1, 2, 3]. A key component for the realization of a practical FBG based sensing system is a low cost interrogation system that can accurately measure the wavelength change of the reflection peak of a FBG. A number of techniques have been developed for this purpose. Among the popular techniques for interrogation of a large number of multiplexing FBG sensors include the use of a broadband optical

DOI: 10.1587/elex.14.20170955
Received September 16, 2017
Accepted September 26, 2017
Publicized October 12, 2017
Copyedited October 25, 2017

source such ASE source or SLED with a tunable optical filter or a tunable laser with an optical detector. The tunable lasers scheme provides a good balance for accuracy, capacity, demodulation speed and cost and as a result is more widely used especially multi-channel wavelength division multiplexed FBG sensing network.

While various FBG demodulation schemes based on a tunable laser source have been developed, the primary task invariably comes to the demodulation algorithm for precise determination of the often slight measured induced wavelength shift from the reflected or transmitted spectrum. In previous works, many demodulation algorithms have been proposed, such as cross-correlation method [4], peak searching method [5, 6, 7], and modified centroid algorithm [8].

However, two reflectance spectrums of FBGs need to be acquired by laser and photodiode in [4]. Then the strain is demodulated by a cross-correlation algorithm. For peak searching method [5, 6, 7], output wavelength of tunable laser need to be tuned by injection current/temperature to search and match the reflected FBG's center wavelength. In [8], rapid wavelength tuning of laser has to be made through FBG's whole spectrum and modified centroid algorithm is utilized for the demodulation of nonequidistantly sampled FBG sensor signals.

For these algorithms to work correctly, tunable laser have to be rapidly tuned through FBG's whole spectrum. Due to long scanning times of wide tuning range, they were not able to use wavelength-division multiplexing for FBG sensing network, especially for tunable lasers which are thermally controlled and are having scanning times on the order of seconds. The response time of the demodulation system will be affected, which is important for most applications that need dynamic, real-time measurements. Such applications include health monitoring of different structures such as floating structures (aircraft fuselage or ship's hull) or for the measurement of mechanical parameters with FBGs embedded in artificial skins, or for medical applications [9, 10, 11].

It remains a great challenge to design an effective algorithm to support rapid response of demodulation system and wavelength division multiplexing of FBG sensing network.

In this paper, a demodulation algorithm based on tunable laser array source is proposed to achieve targeted performance while alleviating the constraints imposed by aforementioned response time, wavelength tuning range of laser and scanning time issues. To implement a fast and accurate demodulation system on demand, a DFB fast tunable laser array is used as key component of the system, which has a tuning speed by injecting current is about 10–30 microseconds much faster than that by the thermal-electric cooler (TEC). In comparison with other algorithms which can work correctly by scanning through FBG's whole spectrum, the algorithm by only scanning 0.4 nm bandwidth of FBG reflected spectrum can enable an accurate demodulation result with error less than ±1 pm. Besides, the scanned spectrum of FBG by tunable laser can be any part of whole FBG spectrum including those regions with relatively low power. Therefore, tunable laser doesn't need to be tuned in relatively wide wavelength tuning range such as 2 nm and scanning times on the order of seconds by thermal control. Output wavelength of tunable laser doesn't need to be tuned to search and match the reflected FBG's

DOI: 10.1587/elex.14.20170955
Received September 16, 2017
Accepted September 26, 2017
Publicized October 12, 2017
Copyedited October 25, 2017

center wavelength. The algorithm can support rapid response of demodulation system and wavelength division multiplexing of FBG sensing network.

2 Principle of algorithm

The system of demodulation is shown in Fig. 1. It includes a tunable DFB-LD (DFB laser diode) array with four tunable channels integrated as light source, a section of fiber containing FBG, a translation stage/moving stage, which is used to supply strain, an optical spectrum analyzer (OSA) and a circulator.

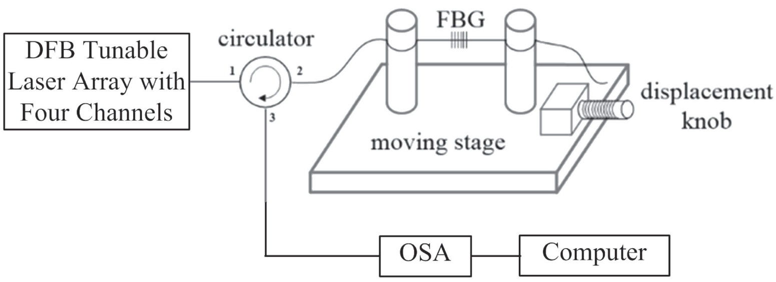

Fig. 1. Schematic of proposed strain sensing system based on four-channel tunable DFB laser array.

FBG possesses filtering characteristic, which can be written as

$$\lambda_B = 2n_{eff}\Lambda \tag{1}$$

where λ_B is the Bragg wavelength, n_{eff} is the effective refractive index of FBG, and Λ is the optical grating period. When the strain is applied on FBG, the Bragg wavelength will shift, which is given by

$$\Delta\lambda_B = 2\Delta n_{eff}\Lambda + 2\Delta n_{eff}\Lambda \tag{2}$$

Based on the formulas above, we will illustrate the demodulation principle of the Bragg wavelength shift. As shows in Fig. 2, the left solid curve is FBG's reflected spectrum in the condition of natural state. The data of the whole reflected spectrum in the natural state is measured by OSA and saved in MATLAB as $\{(\lambda_1, P_1), (\lambda_2, P_2), (\lambda_3, P_3), \ldots\}$. When external strain is applied, the FBG's spectrum is shifted to the right. The wavelength shift of FBG ($\Delta\lambda$) is obtained from the

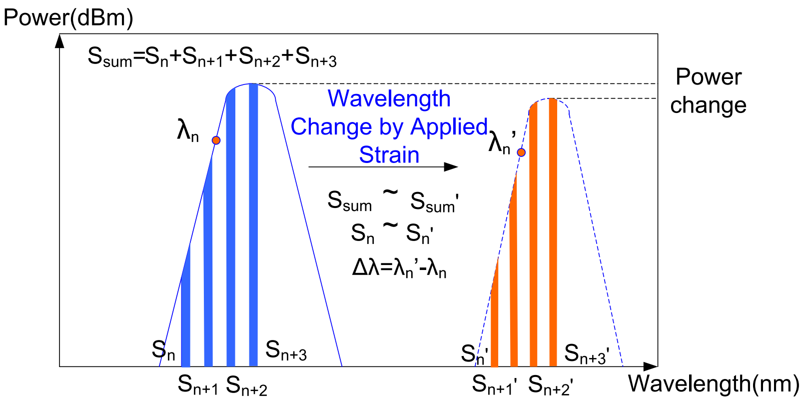

Fig. 2. Schematic of demodulation method by matching corresponding area of reflected power spectrums of FBG sensor.

DOI: 10.1587/elex.14.20170955
Received September 16, 2017
Accepted September 26, 2017
Publicized October 12, 2017
Copyedited October 25, 2017

IEICE Electronics Express, Vol.14, No.20, 1–10

calculated results of λ_n' and λ_n. If the normalized area after wavelength shift (marked in yellow) is the same with area before wavelength shift (marked in blue), it means wavelength change $\Delta\lambda = \lambda_n' - \lambda_n$.

By utilizing tunable laser array with four channels, the FBG's reflected spectrum is scanned and sampled by the laser after wavelength shift. Power values at corresponding wavelengths are acquired. Since there is power variation when the reflected spectrum's wavelength shifts, the acquired power data after the wavelength shift is normalized to offset the power change. After this, power values in the scanned wavelength range are added to reduce the error rate of the algorithm. If the normalized area after wavelength change (marked in yellow) is the same with area before wavelength change (marked in blue), it means wavelength change $\Delta\lambda = \lambda_n' - \lambda_n$.

In Fig. 2, when the external strain is applied and wavelength of FBG's reflected spectrum shifts, by utilizing tunable laser array with four channels, 400 points with 1 pm interval of FBG's reflected spectrum data at different wavelengths are scanned and recorded as: $\{(\lambda'_{1\text{-}1}, P'_{1\text{-}1}), (\lambda'_{1\text{-}2}, P'_{1\text{-}2}), \ldots, (\lambda'_{1\text{-}100}, P'_{1\text{-}100})\}$, $\{(\lambda'_{2\text{-}1}, P'_{2\text{-}1}), (\lambda'_{2\text{-}2}, P'_{2\text{-}2}), \ldots, (\lambda'_{2\text{-}100}, P'_{2\text{-}100})\}$, $\{(\lambda'_{3\text{-}1}, P'_{3\text{-}1}), (\lambda'_{3\text{-}2}, P'_{3\text{-}2}), \ldots, (\lambda'_{3\text{-}100}, P'_{3\text{-}100})\}$, $\{(\lambda'_{4\text{-}1}, P'_{4\text{-}1}), (\lambda'_{4\text{-}2}, P'_{4\text{-}2}), \ldots, (\lambda'_{4\text{-}100}, P'_{4\text{-}100})\}$. Since the data of the whole reflected spectrum in the natural state is measured by OSA and saved in MATLAB, as what is shown in Fig. 2 marked in blue, 400 points with 1 pm interval of FBG's reflected spectrum in natural state are firstly chosen by MATLAB as: $\{(\lambda_1, P_1), (\lambda_2, P_2), \ldots (\lambda_{100}, P_{100})\}$, $\{(\lambda_{101}, P_{101}), (\lambda_{102}, P_{102}), \ldots (\lambda_{200}, P_{200})\}$, $\{(\lambda_{201}, P_{201}), (\lambda_{202}, P_{202}), \ldots (\lambda_{300}, P_{300})\}$, $\{(\lambda_{301}, P_{301}), (\lambda_{302}, P_{302}), \ldots (\lambda_{400}, P_{400})\}$, P_{400} is power value at wavelength λ_{400}.

All of four groups of scanned data points after wavelength shift should be normalized with original data in natural state. The normalization coefficient is:

$$r_n = \frac{P'_n}{P_n} \quad (n = 1 \sim 4) \tag{3}$$

$$r_{average} = \frac{r_1 + r_2 + r_3 + r_4}{4} \tag{4}$$

$r_{average}$ is average normalization coefficient. By normalize the scanned power data points by this ratio, the power change caused by wavelength shift of FBG's reflected spectrum is minimized. After this, power values of the chosen 400 data points of FBG spectrum in natural state are added and compared with sampled power values of FBG's spectrum after wavelength shift by MATLAB to calculate the wavelength change.

By tuning DFB laser array, power values at corresponding wavelength of FBG sensor is scanned and recorded. In order to calculate the area of FBG's reflected spectrum after wavelength shift, the trapezoid equation is utilized as what is shown on Fig. 3. P'_{100} is the 100th power value of the scanned data for one laser channel with the scanned wavelength range of $L = 100$ pm. The G (Gap) is equal to 1 pm. By using equation below, the corresponding area of trapezoid is calculated as what is shown in Fig. 3:

$$S_n' = \frac{(P'_1 + P'_2) \cdot G}{2} + \frac{(P'_2 + P'_3) \cdot G}{2} + \cdots + \frac{(P'_{99} + P'_{100}) \cdot G}{2} \tag{5}$$

DOI: 10.1587/elex.14.20170955
Received September 16, 2017
Accepted September 26, 2017
Publicized October 12, 2017
Copyedited October 25, 2017

IEICE Electronics Express, Vol.14, No.20, 1–10

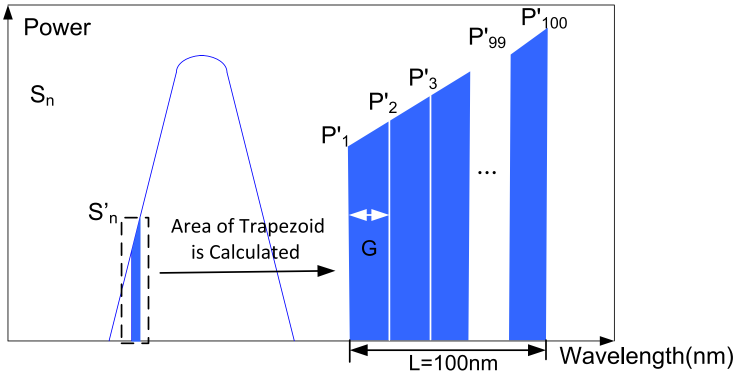

Fig. 3. Schematic of calculating scanned area of trapezoid for one laser channel.

For the other three laser channels, the corresponding area S_{n+1}', S_{n+2}' and S_{n+3}' can be calculated by using the same method. Then

$$S_{sum}' = S_n' + S_{n+1}' + S_{n+2}' + S_{n+3}' \tag{6}$$

Before strain is applied, corresponding area of FBG's reflected spectrum can be calculated with the same method. For the chosen 400 points with 1 pm interval, corresponding area of "S_{sum}" is:

$$S_{sum} = \frac{(P_1 + P_2) \cdot G}{2} + \frac{(P_2 + P_3) \cdot G}{2} + \cdots + \frac{(P_{399} + P_{400}) \cdot G}{2} \tag{7}$$

Corresponding $r_{average}$ is calculated by equations (3–4). By using MATLAB, then S_{sum}' is normalized and compared with S_{sum}, ΔS_n is get by equation below.

$$\Delta S_n = |r_{average} \cdot S_{sum}' - S_{sum}| \tag{8}$$

If the ΔS_n is equal to 0, it means the area difference of corresponding parts of FBG reflected spectrum is 0. It can be concluded that the wavelength shift of FBG caused by applied strain can be get be comparison between wavelengths of the selected two parts of FBG spectrum. If the ΔS_n is not equal to 0, another part of FBG's reflected spectrum in the natural state is chosen by MATLAB and corresponding S_{sum} and $r_{average}$ are calculated again based on the new chosen data points. After compared with S_{sum}', another ΔS_n is get. By using same method, we can get a set of ΔS_n, $\{\Delta S_1, \Delta S_2, \Delta S_3, \ldots, \Delta S_n\}$.

Then the minimum ΔS_n is chosen by MATLAB which means the corresponding area difference of FBG reflected spectrum before and after the strain is applied is minimum. Then by comparing wavelength of the selected two parts of FBG spectrum, the wavelength shift of FBG caused by applied strain can be calculated.

3 Experimental results and discussions

The experimental setup is shown in Fig. 1. The 1550 nm light source is launched into the FBG through a circulator. The laser reflected from the FBG is sent into an OSA, which is used to measure the data of optical spectrum of the FBG sensor. Finally, the measured data are sent into a computer for algorithm processing by MATLAB. The FBG is placed in the moving stage, and the strain applied on the FBG can be regularly changed by controlling the displacement knob.

DOI: 10.1587/elex.14.20170955
Received September 16, 2017
Accepted September 26, 2017
Publicized October 12, 2017
Copyedited October 25, 2017

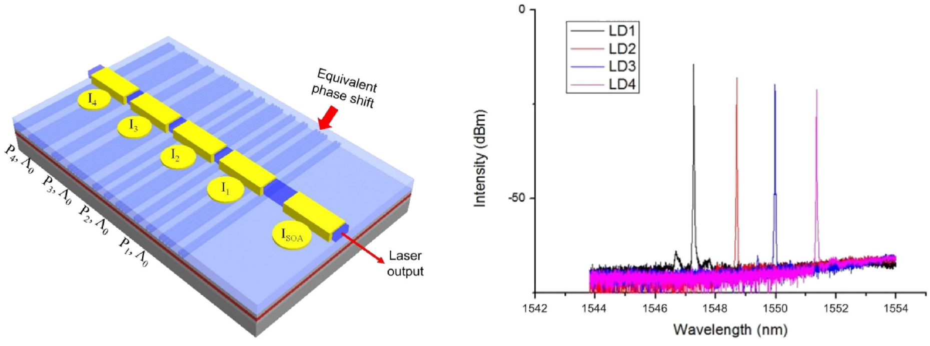

(a) (b)

Fig. 4. Four channel REC technique based DFB laser array. (a) schematic of the laser array design. (b) laser spectrums of the four channel DFB laser array.

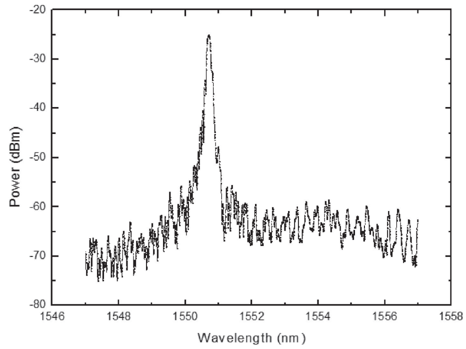

Fig. 5. Reflected spectrum of FBG sensor in natural state.

By tuning injection current of DFB laser diode array, wavelengths of each channel of the array can be tuned [12, 13]. Based on reconstruction-equivalent chirp (REC) technology and through employing phase shift, we have realized four-channel tunable laser array with each laser channel's wavelength can be continuously tuned on a large scale [14, 15]. The characteristic of the tunable DFB-LD array used in the experiment is shown in Fig. 4(a) and Fig. 4(b).

Fig. 5(a) shows FBG's whole reflected spectrum when no strain is applied and are in natural state. By controlling the displacement knob shown in Fig. 1, corresponding external strain is applied and changed, as a result, central wavelength of reflected spectrum of FBG sensor shifts.

By tuning injection current of DFB laser array, each channel's laser wavelength can be tuned to scan 100 pm of FBG's reflected spectrum. Under a certain external strain, 400 pm of reflected spectrum of FBG sensor is scanned and corresponding power values are sampled as what is shown in Fig. 6(a). Then a set of ΔS_n is calculated based on equations discussed above as what shows in Fig. 6(b). ΔS_n is equal to zero means the wavelength shift of FBG ($\Delta\lambda$) is obtained.

In comparison with other algorithms which are based on sampled data points of the FBG's reflected spectrum's power peak or the whole reflected spectrum, sampled data points of only 0.4 nm bandwidth of the FBG reflected spectrum are able for accurate demodulation of the system. Besides, as what is shown in Fig. 7, the sampled part of FBG reflected spectrum can be any part including spectrum

DOI: 10.1587/elex.14.20170955
Received September 16, 2017
Accepted September 26, 2017
Publicized October 12, 2017
Copyedited October 25, 2017

IEICE Electronics Express, Vol.14, No.20, 1–10

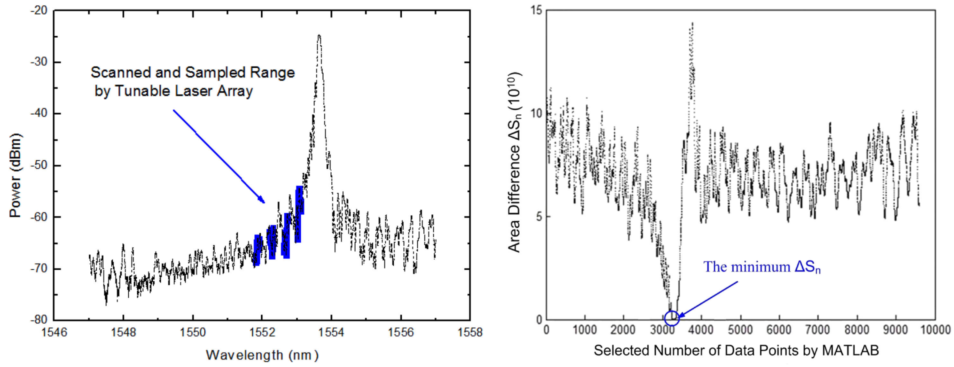

(a) (b)

Fig. 6. Demodulation of wavelength shift of FBG sensor. (a) Blue part of FBG's reflected spectrum after wavelength shift scanned and sampled by tunable laser array. (b) ΔS_n is calculated based on equation (8), different parts of FBG spectrum in natural state are chosen and compared in turn with the scanned part of FBG spectrum marked in blue shown in (a) by MATLAB, the minimum ΔS_n is get when area difference is close to zero.

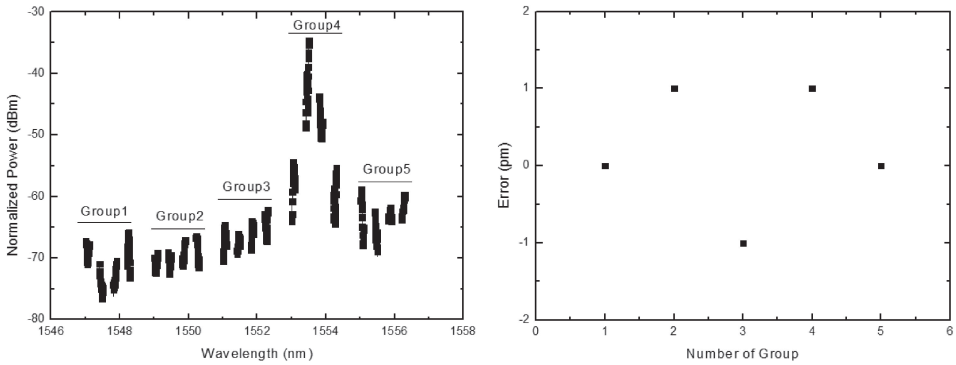

(a) (b)

Fig. 7. Demodulation accuracy analysis when any parts of spectrum with relatively low power is sampled. (a) Five groups of different parts of reflected spectrum of FBG sensor are scanned. (b) Demodulation errors of the five groups.

with relatively low power as what is shown in Fig. 7(a). Five groups of parts of spectrum are scanned and analyzed. The demodulation errors are within ±1 pm as what is shown in Fig. 7(b).

By tuning the tunable DFB laser array to emit laser with different wavelength, we get five groups of data as shown in Fig. 7(a). Each group of data is 4×0.1 nm-bandwidth of FBG's reflected spectrum with same interval, and the maximum error is ±1 pm. The above experiment results show that no matter how far the scanned part of reflected spectrum with 0.4 nm bandwidth are close to the peak of reflected spectrum or away from the peak of reflected spectrum, even if the power of the scanned part are very low or the data are in the nonlinear region, we can accurately demodulate the wavelength shift of FBG.

With 100 $\mu\varepsilon$ for each step, different strain is applied and demodulated as what is shown in Fig. 8. It shows that the wavelength change and the applied strains have

DOI: 10.1587/elex.14.20170955
Received September 16, 2017
Accepted September 26, 2017
Publicized October 12, 2017
Copyedited October 25, 2017

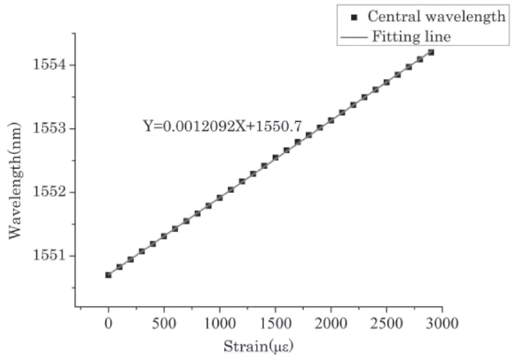

Fig. 8. Experiment results are in good agreement with theoretical results when different strains are applied.

Table I. Measurement error of strain sensing system and corresponding algorithm

Applied strains (number of group)	Theoretical wavelength change	Measured wavelength change by proposed algorithm	Error (pm)
0	/	/	/
1	121 pm	122 pm	+1 pm
2	242 pm	242 pm	+0 pm
3	363 pm	364 pm	+1 pm
4	484 pm	483 pm	−1 pm
5	605 pm	605 pm	0 pm
6	726 pm	725 pm	−1 pm
7	847 pm	846 pm	−1 pm
8	968 pm	967 pm	−1 pm
9	1089 pm	1088 pm	−1 pm
10	1210 pm	1210 pm	0 pm
11	1331 pm	1332 pm	+1 pm

fairly linear relationship with a slope of 1.05 pm/με, which is in good agreement with corresponding theoretical value.

When different strain is applied, central wavelength of FBG sensor is shifted to a different value. Table I shows high accuracy, as expected, the error of the algorithm is within ±1 pm. In the experiment, the data of optical spectrum is not completely continuous smooth, the gap of wavelength is 1 pm. The power cannot maintain a constant from beginning to end, it also has error even if the power has carried on normalization. In summary, the errors is tiny and actually subsistent, the error analysis shows that the algorithm is highly feasible.

Comparison between the demodulation method and other traditional demodulation techniques is shown in Table II [16, 17, 18, 19]. The demodulation system is more simplified than traditional demodulation systems, and has a potential value to be used in low-cost and compact-size commercial applications.

DOI: 10.1587/elex.14.20170955
Received September 16, 2017
Accepted September 26, 2017
Publicized October 12, 2017
Copyedited October 25, 2017

Table II. Comparison between different demodulation techniques

Method	Complexity	Precision	Cost
Tunable F-P filter	complex	1.5 pm (1.25 $\mu\varepsilon$)	High
Unbalanced M-Z interferometer	common	$3.29 \times 10^{-5}\,\varepsilon$ (4.75 nm/ε)	common
Matching grating	common	0.6 $\mu\varepsilon$	common
Edge filtering	complex	1.8 pm (1.5 $\mu\varepsilon$)	High
Our system	simple	1 pm (1.05 pm/$\mu\varepsilon$)	Low

4 Conclusion

A demodulation system based on a novel demodulation algorithm has been implemented. The detailed demodulation methodology has been presented for the algorithm. It is demonstrated that accurate demodulation can be achieved by scanning only 0.4 nm bandwidth of FBG's reflected spectrum and the scanned part can be with relatively low power. The current measurement result suggests for most applications that need dynamic, real-time measurements, the algorithm is able to highly reduce response time of demodulation system and support wavelength-division multiplexing for FBG sensing network.

Acknowledgments

This work is supported by the Natural Science Foundation of Jiangsu Province (BK20160190), the Fundamental Research Funds for the Central Universities (JUSRP11740).

DOI: 10.1587/elex.14.20170955
Received September 16, 2017
Accepted September 26, 2017
Publicized October 12, 2017
Copyedited October 25, 2017